Available online at www.sciencedirect.com
ScienceDirect
Journal of Sound and Vibration 318 (2008) 927–942
JOURNAL OF SOUND AND VIBRATION
www.elsevier.com/locate/jsvi

Lateral dynamic interaction analysis of a train–girder–pier system

H. Xia[a,b,*], W.W. Guo[a], X. Wu[a], Y.L. Pi[b], M.A. Bradford[b]

[a]*School of Civil Engineering & Architecture, Beijing Jiaotong University, Beijing 100044, China*
[b]*Centre for Infrastructure Engineering & Safety, School of Civil & Environmental Engineering, The University of New South Wales, Sydney, NSW 2052, Australia*

Received 7 November 2007; accepted 4 May 2008
Handling Editor: L.G. Tham
Available online 24 June 2008

Abstract

A dynamic model of a coupled train–girder–pier system is developed in this paper. Each vehicle in a train is modeled with 27 degrees-of-freedom for a 4-axle passenger coach or freight car, and 31 for a 6-axle locomotive. The bridge model is applicable to straight and curved bridges. The centrifugal forces of moving vehicles on curved bridges are considered in both the vehicle model and the bridge model. The dynamic interaction between the bridge and train is realized through an assumed wheel-hunting movement. A case study is performed for a test train traversing two straight and two curved multi-span bridges with high piers. The histories of the train traversing the bridges are simulated and the dynamic responses of the piers and the train vehicles are calculated. A field experiment is carried out to verify the results of the analysis, by which the lateral resonant train speed inducing the peak pier-top amplitudes and some other observations are validated.

1. Introduction

The dynamic response of railway bridges subjected to moving trains is one of the fundamental engineering problems requiring solutions in railway design and maintenance. In recent years, with the development of newer railway infrastructure, trains are running increasingly faster, and vehicle loads are becoming increasingly heavier. On one hand, a train running with high speed or carrying heavy loads exerts dynamic impact on bridge structures, causing them to vibrate and thus affecting their working state and serviceability. On the other hand, the safety and stability of train vehicles that traverse the bridges are also affected by the bridge vibrations that they cause and thus in turn become important factors to be included in rational design standards for bridge structures. Moreover, when the loading frequency of the train is equal or close to the natural frequency of the bridge, resonance of the train–bridge system may be induced, which may further intensify the vibration of the vehicles and the structure. Therefore, significant and sustained effort has been

*Corresponding author at: School of Civil Engineering & Architecture, Beijing Jiaotong University, Beijing 100044, China. Tel.: +86 10 82161656; fax: +86 10 51683340.
E-mail address: hxia@center.njtu.edu.cn (H. Xia).

0022-460X/$ - see front matter © 2008 Elsevier Ltd. All rights reserved.
doi:10.1016/j.jsv.2008.05.002

focused on the issue of the dynamic interactions of running vehicles and bridges. The research work on this subject has a long history of more than one hundred years. In the last decade, in particular, a number of analytical models for train–bridge interaction systems have been successively developed by researchers in China and abroad. The fundamental theories of bridge structures under moving trainloads have been published by a number of researchers including Frýba [1], Yang and Yau [2,3], Ju and Lin [4], Fafard et al. [5], and Xia [6]. The dynamic response of large span bridges subjected to moving trains and under the action of wind or earthquake excitations has been reported by Xu and Zhang [7], Diana and Cheli [8], and Xia et al. [9]. Problems concerning multi-span bridges under high-speed train loading have been considered by Cheung et al. [10], Matsuura [11], Klasztorny [12], Xia and Zhang [13], and De Roeck et al. [14]. On the basis of these studies, the vertical and lateral dynamic responses of bridge structures, and the safety and stability of train vehicles during transit, have been studied and many useful results have been contrived. This subject, however, is very complicated, it is influenced by many factors, and there remain some problems that have not been satisfactorily solved hitherto. Most of the previous studies to date have focused on the dynamic interactions between vehicles and the bridge super structure, but the bridge piers have important influences on the lateral vibration of multi-span bridges, especially in mountainous regions where high pier bridges and curved bridges are usually the norm. To the best of the writers' knowledge, although several studies have been reported which consider the influences of centrifugal forces of moving train vehicles on curved bridges [1,6,16], methodologies on the analysis of the dynamic interactions in a train–girder–pier system do not appear to have been published in the open literature.

In this paper, by taking a test train and four real bridges with high piers that support multi-span and simply supported girders as the object of study, a dynamic model for analyzing the vibration of a train–girder–pier system is developed based on the authors' previous work [13]. The centrifugal forces of moving vehicles on curved bridges are considered both in the vehicle model and the bridge model. An assumed wheel-hunting movement is regarded as the lateral excitation and the vertical track irregularity as the vertical excitation to the train–bridge system. The entire histories of the train traversal of the bridges are simulated by computer using real parameters for the vehicles and the bridges. A field experiment for the test train and the four bridges is carried out, in which the lateral displacements of the pier-tops and the accelerations of the vehicle bodies are measured. The vibration behavior of high piers and the dynamic responses of vehicles traversing the bridges are studied herein based on the numerical results and the experimental data.

2. Dynamic model of train–bridge system

When a train moves along a bridge, the train vehicles, bridge girders, piers and their foundations form a complex dynamic interaction system, as shown in Fig. 1. The dynamic analysis model of such a system is composed of the train submodel, the bridge submodel and an assumed wheel–track relationship.

2.1. Train model

The train model consists of several locomotives, passenger coaches, freight wagons, or their combinations. Each vehicle model represents a locomotive, a passenger coach or a freight wagon, which is a complicated

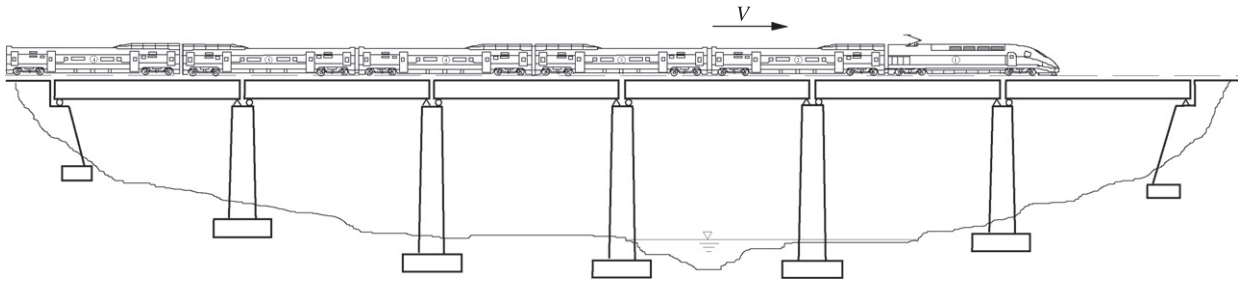

Fig. 1. Dynamic model of train–bridge system.

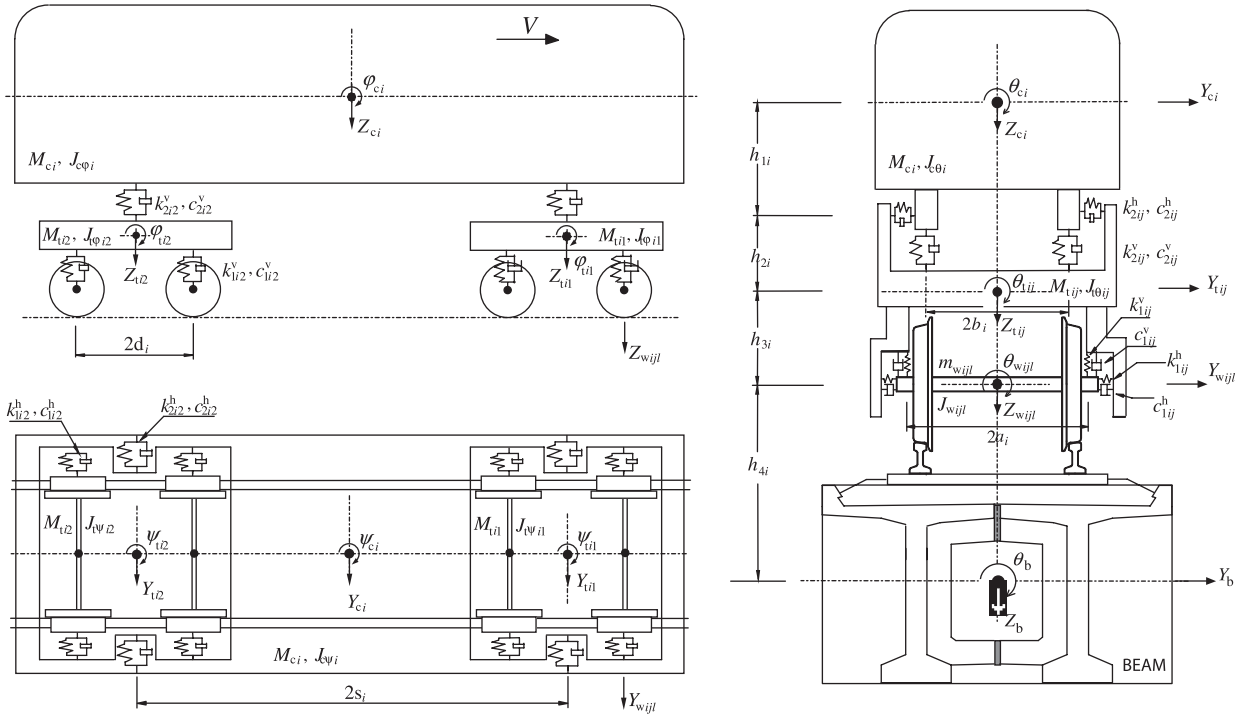

Fig. 2. Dynamic interaction of vehicle and bridge girder.

multi-degree system composed of a car-body, two bogies, four or six wheelsets, and the spring-dashpot suspensions between the three components, as shown in Fig. 2. To simplify the analysis whilst retaining sufficient accuracy, the following assumptions are used in modeling the train vehicle in this study:

(1) The car-body, bogies and wheelsets in each vehicle are regarded as rigid components, neglecting their elastic deformation during vibration. In dealing with bridge vibrations, this assumption is adopted in most research work and has been established as being valid [6–9].
(2) The connections between a bogie and wheelsets are characterized as linear springs and viscous dashpots of the primary suspension system. The horizontal spring stiffness and damping coefficients of them on the *j*th bogie of the *i*th vehicle are denoted as k^h_{1ij} and c^h_{1ij}, and the vertical ones as k^v_{1ij} and c^v_{1ij}, respectively.
(3) The connections between the car-body and bogies are characterized as linear springs and viscous dashpots of the secondary suspension in horizontal direction (k^h_{2ij} and c^h_{2ij}) and vertical direction (k^v_{2ij} and c^v_{2ij}), respectively.

With the above assumptions, the *i*th vehicle body has five degrees of freedom (dofs) to be considered. They are designated by lateral Y_{ci}, rolling θ_{ci}, yawing Ψ_{ci}, vertical Z_{ci} and pitching φ_{ci} movements. The *j*th bogie on the *i*th vehicle has five dofs: the lateral Y_{tij}, rolling θ_{tij}, yawing Ψ_{tij}, vertical Z_{tij} and pitching φ_{tij} movements. For the *l*th wheelset on the *j*th bogie and *i*th vehicle, only three dofs are considered: the lateral Y_{wijl}, rolling θ_{wijl} and vertical Z_{wijl} movements.

Based on these assumptions, the idealized model for a passenger coach or a freight wagon with 2 bogies and 4 wheelsets can therefore be described by 27 dofs, as shown in Fig. 2. Whereas for a locomotive with 2 bogies and 6 wheelsets, the model has 31 dofs.

2.2. Bridge model

The bridge model consists of multi-span girders, piers and their foundations. For straight bridges, the dynamic analysis model reported in Ref. [13] can be used directly.

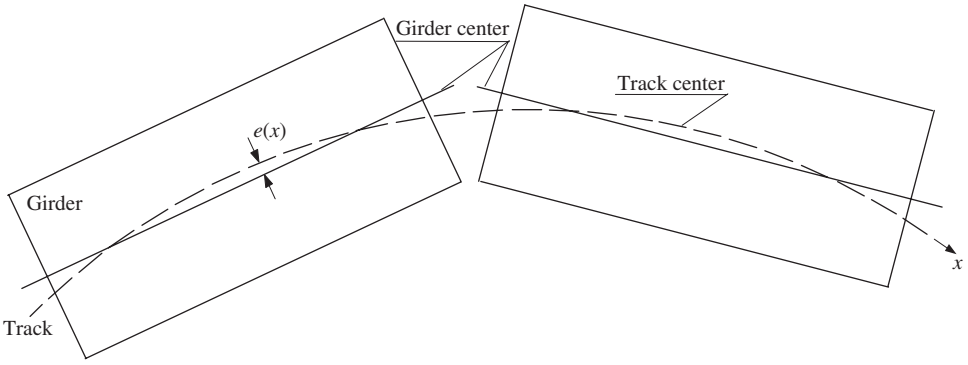

Fig. 3. Relation between the curved track and straight girders.

The curved bridges considered in this study consist of straight girders arranged on railway lines aligned in a curve, as shown in Fig. 3. On these curved bridges, the train moves along the curved track, so that an eccentricity $e(x)$ exists between the longitudinal center of the straight girder and the curved railway track. Owing to this eccentricity, the train induces an additional rotation or torsional moment on the girder, which needs to be taken into account in the model.

The connection between the girders and the piers are by steel rocker bearings, with each girder mounted with fixed bearings at one end and movable ones at the other, as shown in Fig. 1. According to their properties, the rocker bearings are modeled as follows: for movable bearings, the translational displacements in the longitudinal axis x, and the rotational angles about the vertical axis z and the transverse axis y of the girder ends are free, with the other two translational displacements and one rotational angle as the master-and-slave dofs with the pier-tops; for fixed bearings, the rotational angles about the vertical axis z and the transverse axis y of the girder ends are free; with the other three translational displacements and one rotational angle as the master-and-slave dofs with the pier-top.

2.3. Displacement of wheels (linking equations)

It is widely recognized that modeling of wheel–track relationships is one of the key problems in vehicle–bridge interaction system analysis.

There are two models for dealing with the wheel–track relationship. One utilizes the wheel–track contact forces as the interface between the bridge and vehicle models, in which the tangent force is defined from Kalker creep theory from the relative velocity of the wheel and the bridge track, while the normal force is defined by Hertz contact theory from the relative displacement of the wheel and the bridge track. In this model, detailed modeling of the wheel–track contact state is required, from which the contact forces are obtained via iterative calculation, and then input to the bridge and vehicle models as their excitations.

Another model is based on the displacement corresponding relationship. In this model, the relative movement between the wheel and bridge track is assumed as a known quantity, and is input into the train–bridge system for direct solution where neither detailed modeling of wheel–track contact state nor iterative calculation is required, which makes this model much simpler than the previous one.

It is also well recognized that the track irregularities play an important role in the lateral interaction analysis of the vehicle–bridge system; in most studies using this model, therefore, the track irregularities are taken as the self-excitations of the train–bridge system.

In fact, when excited by the track irregularities, the wheel-hunting movement occurs when a vehicle traverses the track, which causes the vehicle to vibrate and thus induce lateral impacts on the bridge. Therefore, if the wheel-hunting movement is known, its data series can also be considered as a significant self-excitation to the lateral vibration of the train–bridge system.

The wheel-hunting movement is not only influenced by the track irregularities, but also by such additional factors as the wheel radius, the worn state of the wheel tread, and the fixing stiffness of the wheels on the bogie. According to the accepted theories of vehicle dynamics, the hunting movement of a wheel can be

expressed approximately as [15–18]

$$y_h(x) = A_h \sin \frac{2\pi V}{L_h} t \tag{1}$$

where A_h is the amplitude of the hunting movement; V is the velocity of wheel; L_h is the wavelength of the hunting movement given by

$$L_h = 2\pi\sqrt{\frac{br_0}{\lambda}} \tag{2}$$

where $2b$ is the transverse distance between the wheel–rail contact point; r_0 is the wheel rolling radius in its central position; λ is the effective conicity of the wheel tire, which is taken as 0.05 for a new wheel and 0.116 for a normal worn one [17]. In China, the ultimate effective conicity for a worn wheel is normally controlled as being 0.15 to ensure its hunting stability [18]. Therefore, the wheel-hunting wavelength may be in the range of 9.06–15.7 m, corresponding to the effective conicities of 0.15 and 0.05, respectively.

Eq. (1) is in accordance with the experimental study in Ref. [15], which shows the main trend that the measured wheel-hunting frequencies increase linearly with the train speed when it is lower than 160 km/h. The study also shows that the measured wheel-hunting amplitudes are mainly between 3 and 4 mm in the same train speed range.

The formula for the hunting movement of a wheel in Eq. (1) is usually adopted in a straight track system. However, this formula is not valid for a curved railway track, because when a wheel rolls on the curved track, the centrifugal force of the vehicle makes the wheel move against the outer rail and thus produces a lateral contact with the track. In this case, the movement of the wheel is controlled by the track irregularities.

Based on the aforementioned assumptions, the wheel-hunting movement is regarded as the lateral excitation and the vertical track irregularity as the vertical excitation to the train–bridge system in this study. Let ϕ^n_{hij}, $\phi^n_{\theta ij}$ and ϕ^n_{vij} denote, respectively, the values of the lateral, rotational and vertical components of the nth bridge mode at the position of the ijlth wheelset, and q_n denote the generalized coordinate of the nth mode. The movements of the wheelset can then be expressed as

$$\begin{Bmatrix} Y_{wijl} \\ \theta_{wijl} \\ Z_{wijl} \end{Bmatrix} = \sum_{n=1}^{N_b} \begin{Bmatrix} q_n[\phi^n_{hijl} + h_{4i}\phi^n_{\theta ijl}] \\ q_n\phi^n_{\theta ijl} \\ q_n[\phi^n_{vijl} + e(x)\phi^n_{\theta ijl}] \end{Bmatrix} + \begin{Bmatrix} Y_h(x_{ijl}) \\ \theta_h(x_{ijl}) \\ Z_s(x_{ijl}) \end{Bmatrix} \tag{3}$$

where N_b is the number of bridge mode shapes concerned, h_{4i} is the vertical distance between the wheel centroid and the shear center of the bridge cross section, e is the eccentricity between the track and the girder center, $\theta_h(x)$ is the rotational displacement induced by the lateral hunting movement $Y_h(x)$ of the wheel with conical tread, $Z_s(x)$ is the vertical track irregularity along the track, and x_{ijl} is the coordinate of the ijlth wheelset along the bridge deck. The relationship between the wheelset displacement and the bridge movement is illustrated in Fig. 4. In Eq. (3), a sole generalized coordinate q_n is used to represent different vibration modes, with the aid of the modal shape components $\phi_h{}^n$, $\phi_\theta{}^n$ and $\phi_v{}^n$, which play different roles in different modes. For example, the lateral component $\phi_h{}^n$ contributes most, while the others contribute lesser or even not at all to the vibration mode which is mainly in lateral movement.

Therefore, the movements of the wheelsets are not independent and need not be included in the equations of motion for the train–girder–pier system. The role of Eq. (3) is to link up the train model with the bridge model to form the system equations.

2.4. Centrifugal forces

When a train traverses a curved bridge, centrifugal forces exist which act on the vehicle car bodies, bogies and wheelsets, which are further transmitted onto the bridge structure through the wheels. The status of the train vehicle on the girder of the curved bridge is illustrated in Fig. 5.

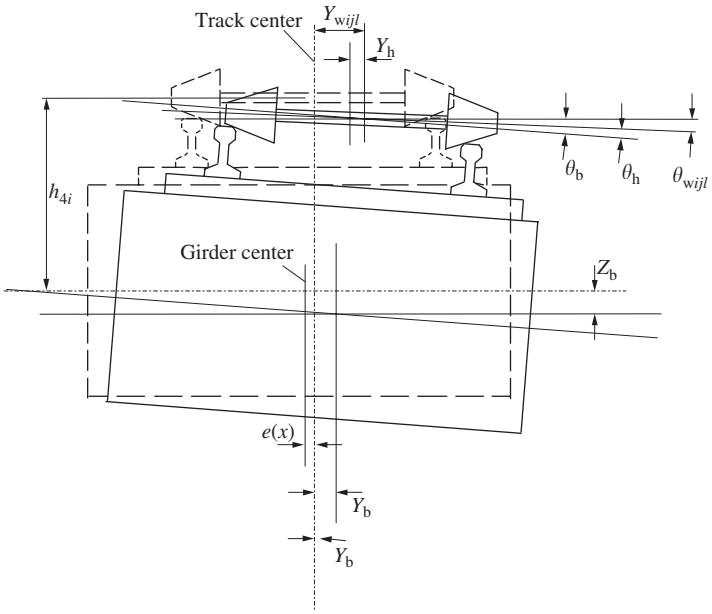

Fig. 4. Relation between wheelset displacement and bridge movement.

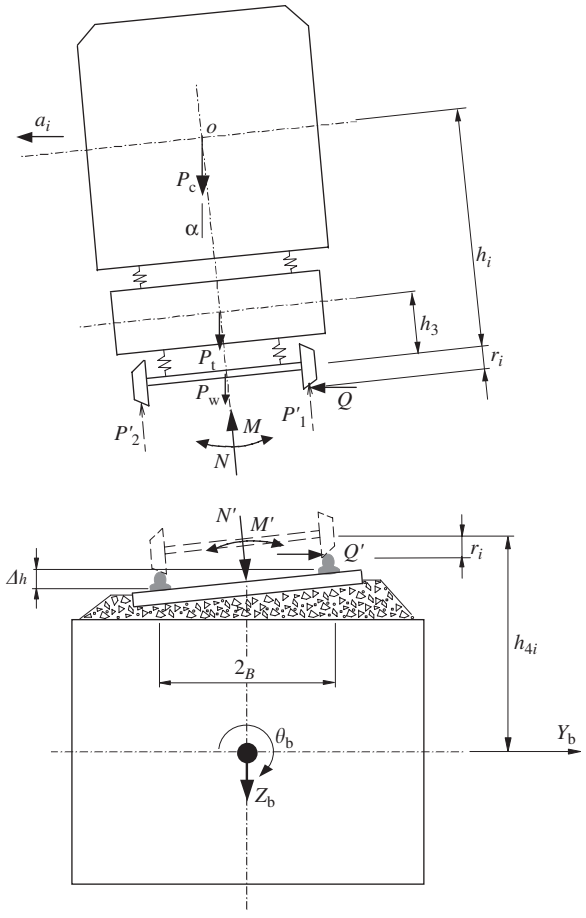

Fig. 5. Centrifugal forces acting on the vehicle and the girder.

The centrifugal forces acting on the car-body, bogies and wheelsets can be directly written as

$$\begin{cases} \text{Car-body}: & F_{ci}^{R} = -M_{ci}a_i = -M_{ci}\dfrac{V^2}{R} \\ \text{Bogie}: & F_{tij}^{R} = -M_{tij}a_i = -M_{tij}\dfrac{V^2}{R} \\ \text{Wheelset}: & F_{wijl}^{R} = -m_{wijl}a_i = -m_{wijl}\dfrac{V^2}{R} \end{cases} \tag{4}$$

where M_{ci}, M_{tij} and m_{wijl} are the mass of the car-body, bogie and wheelset, respectively, a_i is the centrifugal acceleration, V the train speed, and R the radius of curvature of the railway track.

As shown in Fig. 5, for the curved bridge, the forces of the vehicle acting on the bridge include: the normal force N', the lateral force Q' and the moment M'. The nth modal centrifugal force F_{bn}^{R} of the train vehicles on the bridge is the summation of the generalized forces transmitted from all wheelsets, which can be expressed as

$$\begin{aligned} F_{bn}^{R} = \sum_{i=1}^{N_v}\sum_{j=1}^{2}\sum_{l=1}^{N_{wi}}\Bigg\{ & \left[\left(\frac{M_{ci}}{2N_{wi}} + \frac{M_{tij}}{N_{wi}} + m_{wijl}\right)\Phi_{h\theta ijl}^{n} + \left(\frac{M_{ci}h_i}{2N_{wi}} + \frac{M_{tij}h_3}{N_{wi}}\right)\phi_{\theta ijl}^{n}\right]\frac{V^2}{R} \\ & - \left[\frac{M_{ci}}{2N_{wi}}(h_i + r_i) + \frac{M_{tij}}{N_{wi}}(h_3 + r_i) + m_{wijl}r_i\right]\phi_{\theta ijl}^{n} g\frac{\Delta h}{2B}\Bigg\} \end{aligned} \tag{5}$$

where N_v is the number of vehicles on the bridge, N_{wi} is the number of wheelsets on each bogie of the ith vehicle, ${\Phi_{h\theta ij}}^{n} = {\phi_{hijl}}^{n} + h_{4i}{\phi_{\theta ijl}}^{n}$; r_i is the radius of the wheelset, g is the gravity acceleration, Δh is the outer rail cant of the curved track, as shown in Fig. 5. The detailed derivation of Eq. (5) is lengthy, and can be found in Ref. [6].

2.5. Equations of motion of train–bridge system

By assuming that the amplitude of vibration of the bridge and each component in a vehicle is small, using the equilibrium conditions, and combining the train model, bridge model and the train–bridge linking equations, the coupled equations of motion for the bridge–train system have been established in Ref. [13] as

$$\begin{bmatrix} \mathbf{M}_{vv} & 0 \\ 0 & \mathbf{M}_{bb} \end{bmatrix}\begin{Bmatrix} \ddot{\mathbf{X}}_v \\ \ddot{\mathbf{Q}}_b \end{Bmatrix} + \begin{bmatrix} \mathbf{C}_{vv} & \mathbf{C}_{vb} \\ \mathbf{C}_{bv} & \mathbf{C}_{bb} \end{bmatrix}\begin{Bmatrix} \dot{\mathbf{X}}_v \\ \dot{\mathbf{Q}}_b \end{Bmatrix} + \begin{bmatrix} \mathbf{K}_{vv} & \mathbf{K}_{vb} \\ \mathbf{K}_{bv} & \mathbf{K}_{bb} \end{bmatrix}\begin{Bmatrix} \mathbf{X}_v \\ \mathbf{Q}_b \end{Bmatrix} = \begin{Bmatrix} \mathbf{F}_v \\ \mathbf{F}_b \end{Bmatrix} \tag{6}$$

where $\mathbf{X}_v$, $\dot{\mathbf{X}}_v$ and $\ddot{\mathbf{X}}_v$ are, respectively, the displacement, velocity and acceleration sub-vectors of the ith vehicle, $\mathbf{Q}_b$, $\dot{\mathbf{Q}}_b$ and $\ddot{\mathbf{Q}}_b$ are the generalized displacement, velocity and acceleration sub-vectors of the bridge, respectively, $\mathbf{M}_{vv}$, $\mathbf{K}_{vv}$ and $\mathbf{C}_{vv}$ are the sub-mass, sub-stiffness and sub-damping matrices of vehicles, respectively, $\mathbf{M}_{bb}$, $\mathbf{K}_{bb}$ and $\mathbf{C}_{bb}$ are the generalized sub-mass, sub-stiffness and sub-damping matrices of bridge structure, respectively. The sub-stiffness and sub-damping matrices are marked with subscripts "vb" or "bv" to denote the interaction between the bridge and the vehicles, respectively. Details of these sub-vectors and the submatrices are the same as the corresponding ones in Ref. [13].

This model has been successfully used in the analysis of railway bridges subjected to high-speed trains [13] and can be used directly for the case of straight bridges with high piers. When it is applied to curved bridges, the sub-force vectors $\mathbf{F}_v$ of vehicle and $\mathbf{F}_b$ of bridge structure should include the centerifugal forces as follows.

2.5.1. Sub-force vectors of vehicles

The force vector of vehicles can be expressed as [13]

$$\mathbf{F}_v = [\,\mathbf{F}_{v1} \quad \mathbf{F}_{v2} \quad \cdots \quad \mathbf{F}_{vN_b}\,]^{\mathrm{T}} \tag{7}$$

where $\mathbf{F}_{vi}$ is the sub-force vector of the ith vehicle given by

$$\mathbf{F}_{vi} = [\,\mathbf{F}_{ci} \quad \mathbf{F}_{t_1 i} \quad \mathbf{F}_{t_2 i}\,]^{\mathrm{T}} \tag{8}$$

in which $\mathbf{F}_{ci}$ is the vector of forces acting on the car-body, it normally represents the external forces such as wind, seismic and centrifugal forces. When only the centrifugal force $\mathbf{F}_{bn}^{R}$ acting on the car-body is considered, it can be expressed as

$$\mathbf{F}_{ci} = [\mathbf{F}_{ci}^{R} \quad 0 \quad 0 \quad 0 \quad 0]^{\mathrm{T}} \tag{9}$$

Also in Eq. (8), $\mathbf{F}_{t_1 i}$ and $\mathbf{F}_{t_2 i}$ are the force vectors of the front and rear bogies, respectively. They include the forces transmitted from the wheels through the primary springs and dashpots, and the external forces. When the centrifugal force $\mathbf{F}_{t_j i}^{R}$ acting on the bogie is considered, it can be expressed as

$$\mathbf{F}_{t_j i} = \sum_{l=1}^{N_{wi}} \begin{cases} k_{1ij}^{h} Y_h(x_{ijl}) + c_{1ij}^{h} \dot{Y}_h(x_{ijl}) + F_{tij}^{R} \\ 2a_i^2[k_{1ij}^{v}\theta_h(x_{ijl}) + c_{1ij}^{v}\dot{\theta}_h(x_{ijl})] - h_{4i}[k_{1ij}^{h} Y_h(x_{ijl}) + c_{1ij}^{h}\dot{Y}_h(x_{ijl})] \\ 2\eta_l d_i[k_{1ij}^{h} Y_h(x_{ijl}) + c_{1ij}^{h}\dot{Y}_h(x_{ijl})] \\ k_{1ij}^{v} Z_s(x_{ijl}) + c_{1ij}^{v}\dot{Z}_s(x_{ijl}) \\ 2\eta_l d_i[k_{1ij}^{v} Z_s(x_{ijl}) + c_{1ij}^{v}\dot{Z}_s(x_{ijl})] \end{cases} \quad (j = 1, 2) \tag{10}$$

where η_l is the sign function with $\eta_l = 1$ when the lth wheel is in the front bogie and $\eta_l = -1$ when it is in the rear bogie.

2.5.2. Sub-force vectors of bridge

The modal load vector of the bridge can be expressed as [13]

$$\mathbf{F}_b = [F_{b1} \quad F_{b2} \quad \cdots \quad F_{bN_b}]^T \tag{11}$$

When the centrifugal force F_{bn}^{R} of the train vehicles on the bridge is considered, the nth component of the modal load vector becomes

$$\begin{aligned} F_{bn} = \sum_{i=1}^{N_v}\sum_{j=1}^{2}\sum_{l=1}^{N_{wi}} & \{(\phi_{hijl}^{n} + h_{3i}\phi_{hijl}^{n})k_{1ij}^{h} Y_h(x_{ijl}) + 2\phi_{\theta ijl}^{n} k_{1ij}^{v} a_i^2 \theta_h(x_{ijl}) + [\phi_{vijl}^{n} + e(x)\phi_{\theta ijl}^{n}]k_{1ij}^{v} Z_s(x_{ijl}) \\ & + [\phi_{vijl}^{n} + e(x)\phi_{\theta ijl}^{n}]g[m_{wijl} + (0.5M_{ci} + M_{tij})/N_{wi}\} + F_{bn}^{R} \end{aligned} \tag{12}$$

As mentioned in Ref. [13], the entries in the mass, stiffness and damping matrices are the functions of train velocity V and time t. When the train traverses the bridge, these elements are always changing along it with the shift of wheel positions of the train vehicles. Thus Eq. (6) is actually a second-order linear nonhomogeneous differential equations with time-varying coefficients. In this study, these equations are solved using the Newmark implicit integral algorithm with $\beta = 1/4$. A computer code was written based on the formulation derived above and was employed to analyze the case study reported below.

3. Case study

3.1. Bridges and test train

There are four multi-span single-track bridges with simply supported girders and high piers considered in the case study. The bridges are located on the Chengdu-Kunming Railway in Southwest China, along which the Mimalong Bridge (Fig. 6a) and the Xiaba Bridge are straight bridges, and the Miandian Bridge (Fig. 6b) and the Xihe Bridge are curved bridges. The main parameters of the four bridges are given in Table 1. As in total there are 24 beams with five types and 20 piers with different heights and foundations in the analysis, the amount of data for the bridges, such as the cross sectional dimensions of the beams and piers, are too large to be listed in this paper, and the details can be found in [19].

ANSYS software was employed in establishing the finite element model of the four bridges. For the straight bridges and the curved bridges consisting of straight girders arranged on curved railway lines, the girders and piers were all discretized by using beam elements, and the secondary loads on the bridge distributed on the

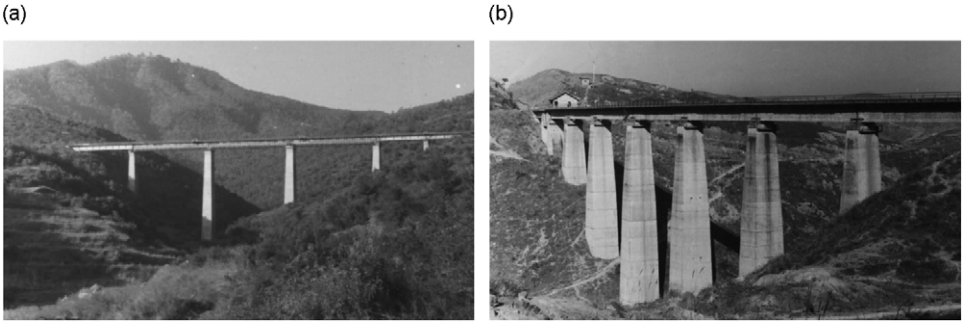

Fig. 6. The bridges under in study: (a) Mimalong bridge and (b) Miandian bridge.

Table 1
Bridge parameters

Bridge	Mimalong	Xiaba	Miandian	Xihe
Span (m)	$1\times32+3\times44+2\times24$	$1\times32+1\times64+4\times32$	7×20	$2\times32+1\times24+2\times32$
Pier height (m)	30, 55, 41, 30, 15	12, 38, 32, 28, 24	28, 39, 41, 40, 32, 19	25, 37, 35, 29
Foundation	Spread	Spread	Spread	Caisson or spread
Curve radius (m)	∞	∞	450	500
Cant (mm)	/	/	55	75

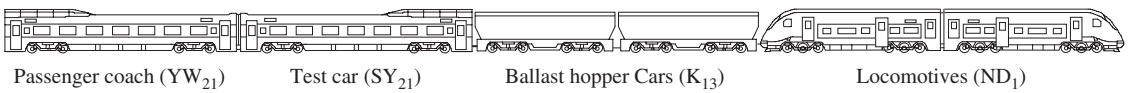

Fig. 7. Composition of the test train.

girders as supplementary masses. The track–ballast system, including that of curved track with cant, was modeled by block elements, to take into account the vertical, lateral and shearing stiffness of the ballast.

The natural vibration properties of the bridges were analyzed and there are 40 frequencies and mode shapes altogether obtained for each multi-span bridge, and were included in the calculation. For multi-span simply supported bridges with high piers of this type, the lowest vibration modes are mainly the lateral movement of the piers. The calculated natural frequencies of some high piers of the two straight bridges from the FEM models are listed in Table 3; the others can be found in Ref. [19].

The train model used in this case study is a test train composed of, successively, two diesel locomotives (ND_1), two ballast hopper cars (K_{13}), a test car (SY_{21}) and a passenger coach (YW_{21}), as illustrated in Fig. 7. The main parameters of the train vehicles are listed in Table 2.

To physically study the dynamic responses of the vehicles and bridges and their interactions, and to validate the calculated results and the practicability of the analysis procedure, the field experiment was carried out for the four bridges and the test train. In the course of the experiment, the lateral displacements of the pier-tops (measured by CD-7 vibration pickups) and the lateral accelerations of the test car-body (by YD-12 accelerometers) were recorded simultaneously while the train moved on the bridge, with about 20 trials conducted for each bridge and 83 trials in total (namely, 20 trials for every pier and 83 trials for the car). The train speeds in the experiment ranged from 9 to 83 km/h. Fig. 8 shows the test train traversing the Xihe Bridge during the experiment.

3.2. Calculation results and their comparisons to experimental data

The entire histories of the test train passing on the bridges were calculated by computer simulation, using the measured parameters for the bridges and the test train. The wavelength of the wheel-hunting movement

Table 2
Vehicle parameters of the test train

Vehicle type	ND_1	K_{13}	SY_{21}	YW_{21}
Self weight (kN)	1284	816	684	624
Tonnage (kN)	/	612	134	134
Full vehicle length (m)	16.920	12.046	21.975	21.975
Rated distance between bogies (m)	8.60	8.00	15.73	15.73
Wheelbase (m)	2.10	1.72	2.44	2.44
Number of wheelsets on each bogie	3	2	2	2
Axle load (kN)	214	204	171	156

Fig. 8. Test train on the Xihe Bridge during experiment.

was taken as 10 m with respect to the effective conicity of worn wheels [17], and the amplitude as 3.5 mm which is the median value in reference to the measured ones [15]. The train speed range in the calculation is 10–120 km/h for straight bridges and 10–90 km/h for curved ones. The damping ratios for the bridges were taken as 0.02 for concrete structures and 0.005 for steel structures, and the integration time interval was taken as 0.002 s.

Since the dynamic interaction between the train and bridge girders has been reported in previous work, the following discussion concentrates mainly on the dynamic responses of the bridge piers and the train vehicles.

3.2.1. Responses of bridge piers

Fig. 9(a) shows the calculated time history curve for the lateral pier-top displacement response of Pier III of the Mimalong bridge, when the train traverses the bridge at 30 km/h, and Fig. 9(b) the measured one for the same pier with the train speed of 32.5 km/h. The figures indicate that the calculated and the measured curves display good correlation. From the curves, one can find the different amplitudes that reflect the influences of the locomotives with heavier wheel-loads and the vehicles with lighter loads.

Fig. 10 compares the calculated and the measured time histories for the lateral pier-top displacements for Pier III of the Xihe bridge with the train speeds of 50 and 48.1 km/h, respectively. The calculated and measured pier-top displacement histories also show quite good agreement for this curved bridge. The figure shows that in deference to the straight bridges, the pier-top displacement curves of the curved bridge contain two main components: the lower frequency component induced by the centrifugal forces and the higher frequency component induced by the wheel-hunting excitations.

Shown in Figs. 11–14 are the distributions of the maximum lateral pier-top displacements versus train speed, where the calculated curves and the measured ones are given for comparison. The results show that the

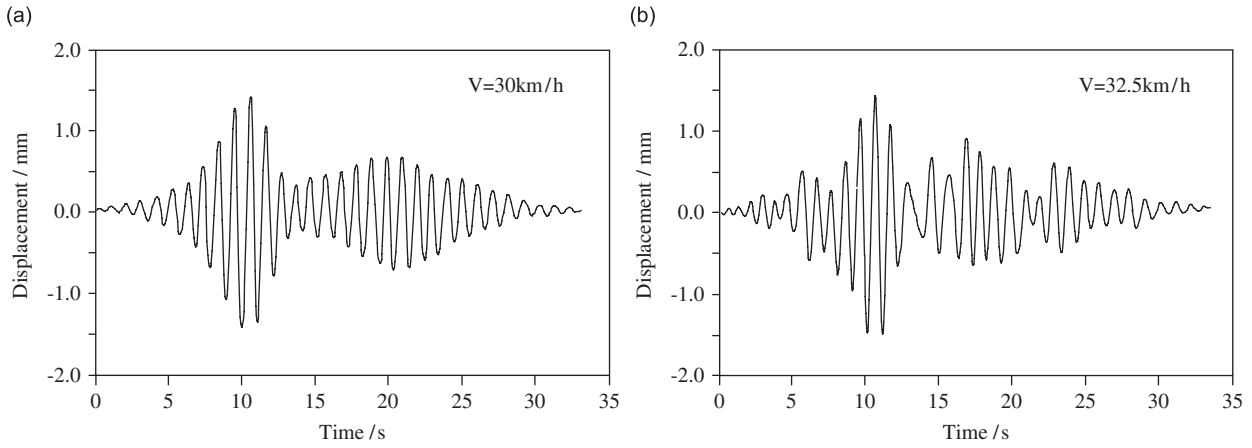

Fig. 9. Typical pier-top displacement of Mimalong Bridge (straight): (a) calculation and (b) measurement.

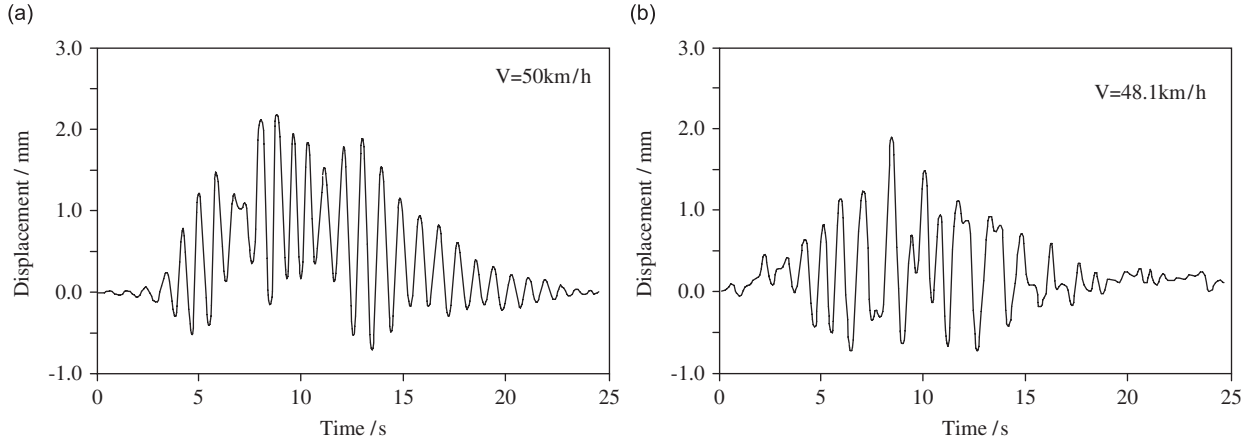

Fig. 10. Typical pier-top displacement of Xihe Bridge (curved): (a) calculation and (b) measurement.

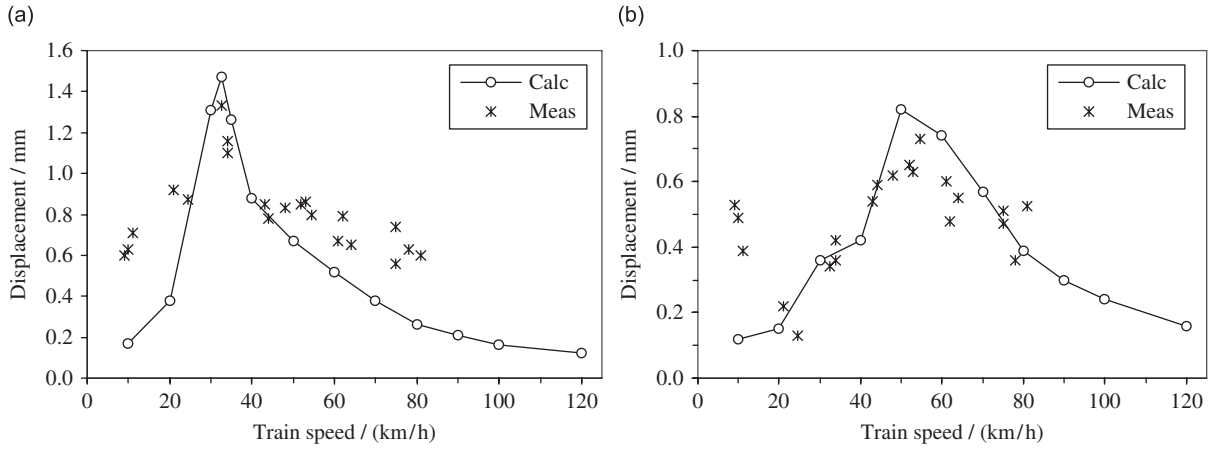

Fig. 11. Pier-top displacement of Mimalong Bridge versus train speed: (a) Pier III and (b) Pier IV.

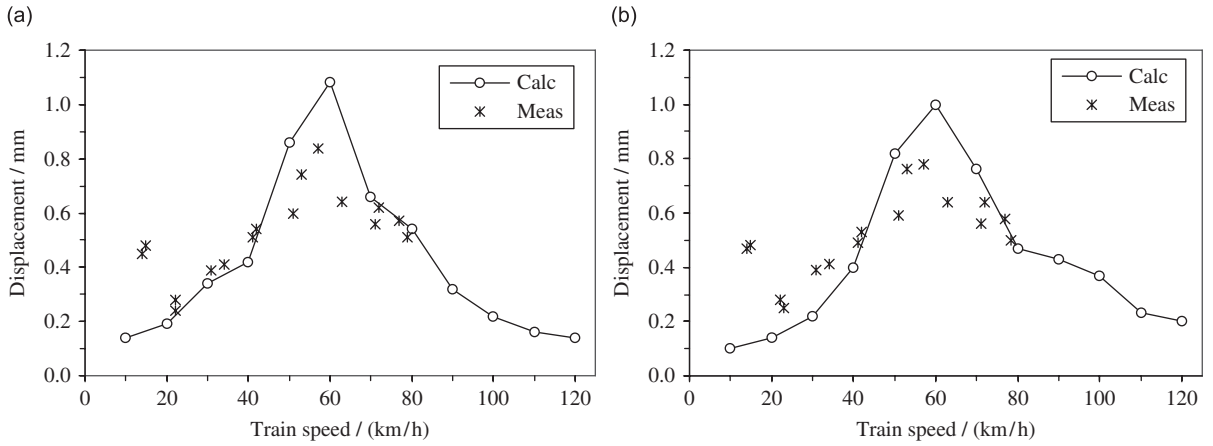

Fig. 12. Pier-top displacement of Xiaba Bridge versus train speed: (a) Pier IV and (b) Pier V.

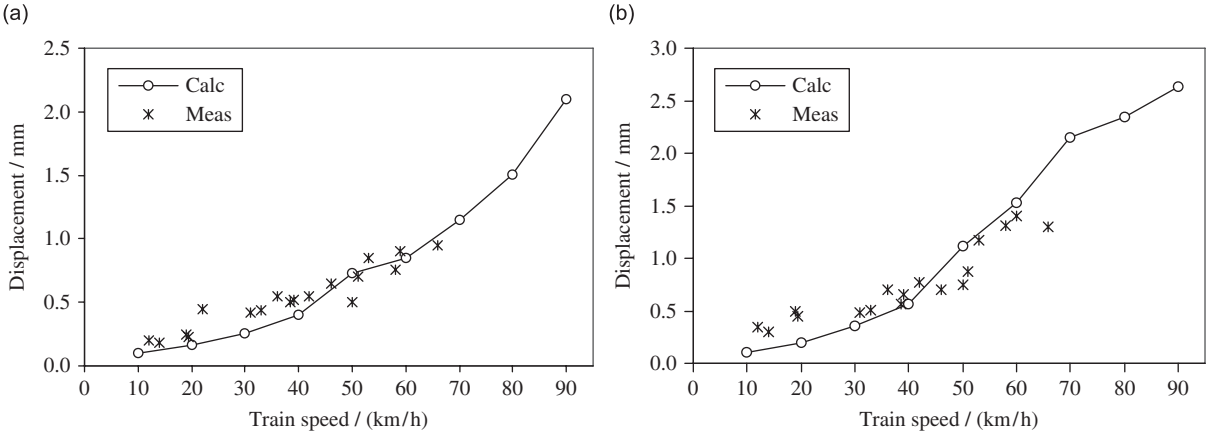

Fig. 13. Pier-top displacement of Miandian Bridge versus train speed: (a) Pier III and (b) Pier IV.

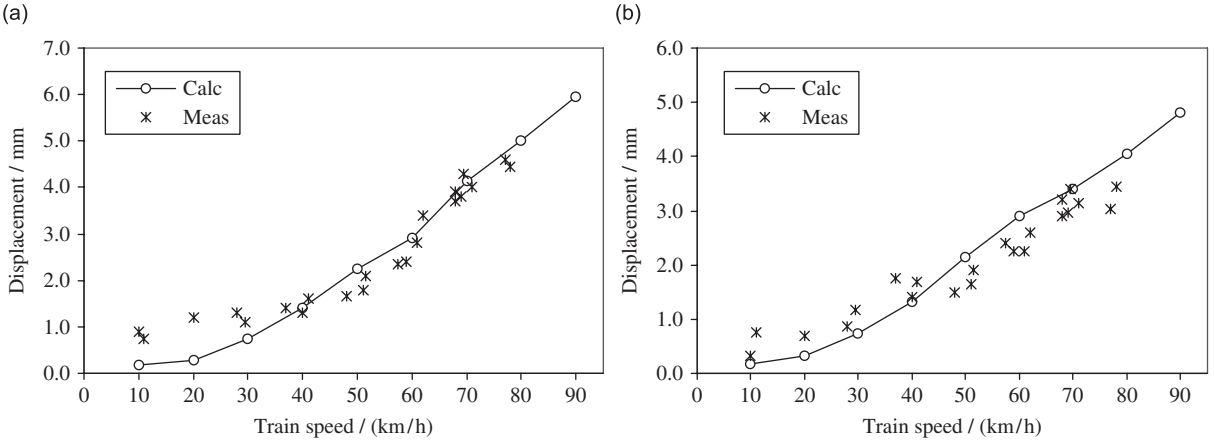

Fig. 14. Pier-top displacement of Xihe Bridge versus train speed: (a) Pier III and (b) Pier IV.

Table 3
Comparison of measured and calculated results

Bridge name	Mimalong				Xiaba		
Pier number	2	3	4	5	3	4	5
Measurement							
Frequency (Hz)	1.98	1.05	1.43	2.02	2.11	1.88	1.96
Peak pier-top displacement (mm)	0.60	1.33	0.75	0.61	0.39	0.95	0.76
Train speed (km/h)	62.6	32.2	55.0	61.7	70.9	54.0	56.9
Calculation							
Frequency (Hz)	2.14	1.08	1.59	2.19	2.14	1.82	1.88
Peak pier-top displacement (mm)	0.74	1.47	0.86	0.71	0.54	1.19	1.01
Train speed (km/h)	70	32.5	50	70	70	60	60

calculated distributions are in accordance with the corresponding measured ones, and the following observations can be concluded from the figures.

For the straight bridges shown in Figs. 11 and 12, peak pier-top displacements occur at certain train speeds. Table 3 lists the measured and the calculated results for the natural frequencies and the peak pier-top displacements of the two straight bridges, and the corresponding train speeds at which the peak displacements occur. These results can help to better understand the mechanism of the peak displacement occurrence. It shows that wheel hunting is the main self-excitation of the lateral oscillations of the train–girder–pier system under moving trainloads. Owing to the influences of the hunting frequency, the vibration of straight bridge piers varies with the train speed. At a certain train speed, the hunting frequency nears the natural frequency of a pier, and resonance for this pier is induced, which makes the amplitude of the pier reach its peak. The train speed when this occurs is the so-called lateral resonant speed. The lateral resonant train speed is thus related to the natural frequency of the pier and the hunting wavelength of the vehicle moving on the bridge. It should be noted that for such multi-span simply supported bridges, whose piers and beams are coupled with each other, and for a train composed of several different locomotives and vehicles, the responses of the piers are complicated. It can be seen from Table 3 that the wheel-hunting wavelengths deduced from the measured results are between 7.98 and 10.54 m, while the calculated results are not exactly at the resonant cases, and so the formula $L_h = V/f$ can only give an approximate estimation of the resonant train speed. The complexity of this problem has been explained in Ref. [20].

In deference to the straight bridges, there is no resonant train speed associated with a peak lateral pier-top displacement of the curved bridge. For all the piers, the pier-top displacements increase when the train speeds become higher, as shown in Figs. 13 and 14. This is because for curved bridges, the centrifugal forces of the train vehicles represent the main loading for the lateral pier-top displacements, while the effect of the wheel-hunting movement becomes a secondary loading.

3.2.2. Response of vehicle accelerations

Figs. 15(a)–(d) show the distributions of the car-body accelerations versus train speed when the test train traverses the four bridges. Both the calculated and the experimental results show the same main trend that the car-body accelerations become greater with the increase of train speed, and the accelerations of the car-body on curved bridges are slightly greater than those on straight bridges.

The physically measured frequencies of the lateral oscillations of the research car-body are plotted in Fig. 16, which shows the distribution of the frequencies with respect to the train speeds. The main trend for these frequencies versus the train speed can be regressed as a linear distribution:

$$F_w(V) = 0.02737V \tag{13}$$

where V is the train speed in km/h. From this equation, and according to Eq. (1), the hunting wavelength of the vehicle can be estimated as 10.15 m. This wavelength is approximately equal to that adopted in the calculation.

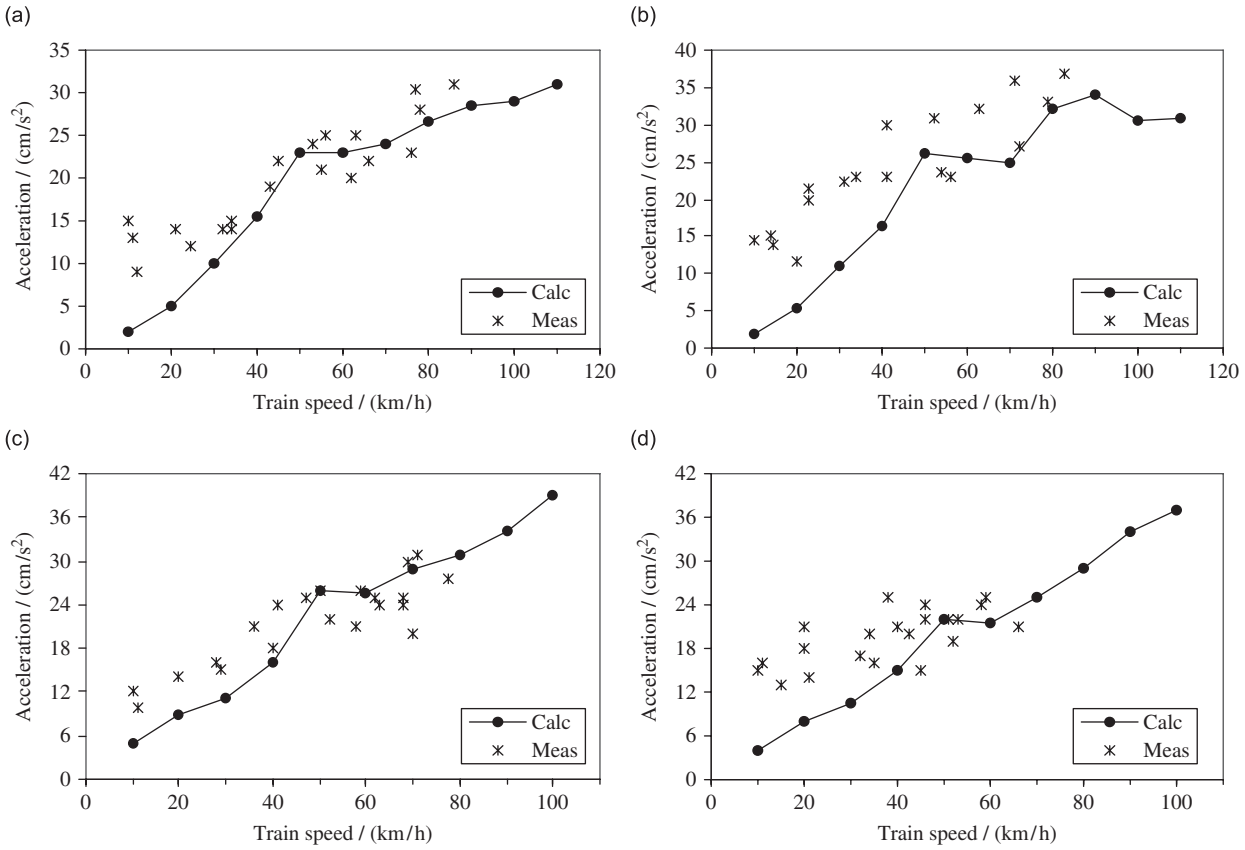

Fig. 15. Car-body accelerations of test car versus train speed: (a) Mimalong bridge, (b) Xiaba bridge, (c) Miandian bridge and (d) Xihe bridge.

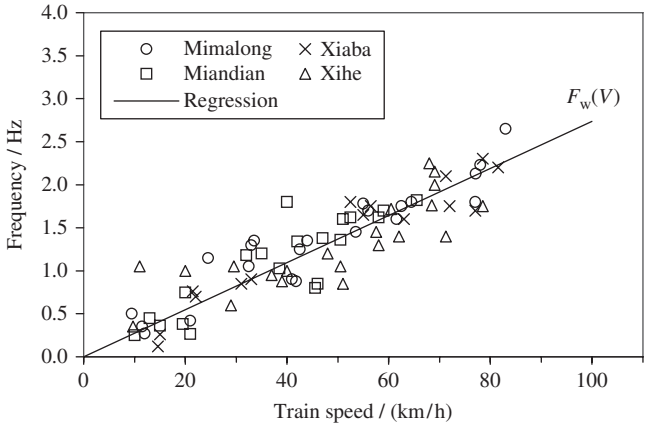

Fig. 16. Distribution of train vehicle frequencies versus train speed.

4. Conclusions

The following conclusions have been drawn from the numerical calculations and the field tests:

(1) The dynamic model of the train–girder–pier system and the computer simulator solution of the dynamic responses of the vehicles and bridge piers can elucidate the main vibration behavior of the vehicles and the piers. The calculated results agree well with those obtained in the field tests.

(2) Wheelset hunting is the main self-exciting source of the lateral oscillations of V–G–P system under moving trains. Owing to the influences of the hunting frequency, the vibration of straight bridge piers is related to the train speed in such a way that at a certain train-speed, the hunting frequency becomes close to the natural frequency of a pier and so resonance is induced, which makes the amplitude of the pier reach a peak value. The lateral resonant train speed influences greatly the natural frequency of the pier and the hunting wavelength of the vehicle moving on the bridge.
(3) For curved bridges, train centrifugals are the main loads that induce the lateral displacements of the bridge piers, while the effect of the wheel-hunting movement becomes a secondary factor. Unlike straight bridge, there is no resonant train speed for curved bridges; the displacements of pier-tops increase with the train speed.
(4) With an increase of train speed (whether on a straight bridge or on a curved one), the oscillation of the car-body becomes greater in frequency as well as in amplitude of its accelerations. The accelerations of the car-body on curved bridges are slightly greater than those on straight bridges.

This paper has proposed a dynamic model of a coupled train–girder–pier system to simulate the lateral vibration response for straight or curved railway bridges subject to moving trains, and the calculated results obtained from the model were verified with the field measurements. Further parametric studies will be performed by this model to determine the key factors that affect the lateral vibration behavior of the system.

Acknowledgements

This study is sponsored by the National Natural Science Foundation of China (50538010, 90715008), the Natural Science Foundation of Beijing (8082021) and the Flander (Belgium)-China Bilateral Project (BIL07/07).

References

[1] L. Frýba, *Vibration of Solids and Structures under Moving Loads*, Thomas Telford, London, 1999.
[2] Y.B. Yang, J.D. Yau, Vehicle–bridge interaction element for dynamic analysis, *Journal of Structural Engineering-ASCE* 123 (11) (1997) 1512–1518.
[3] J.D. Yau, Y.B. Yang, *Theory of Vehicle– Bridge Interaction for High Speed Railway*, DNE Publisher, Taipei, 2002.
[4] S.H. Ju, H.T. Lin, Resonance characteristics of high-speed trains passing simply supported bridges, *Journal of Sound and Vibration* 267 (2003) 1127–1141.
[5] M. Fafard, Mallikarjuna, M. Savard, Dynamics of bridge–vehicle interaction, *Proceedings of the EURODYN'93, Trondheim, Norway*, Vol. 2, Balkema, Rotterdam, 1993, pp. 951–960.
[6] H. Xia, *Dynamic Interaction of Vehicles and Structures*, Science Press, Beijing, 2005.
[7] Y.L. Xu, N. Zhang, Vibration of coupled train and cable-stayed bridge system in cross wind, *Journal of Engineering Structures* 26 (2004) 1389–1406.
[8] G. Diana, F. Cheli, Dynamic interaction of railway systems with large bridges, *Vehicle System Dynamics* 18 (1989) 71–106.
[9] H. Xia, Y.L. Xu, T.H.T. Chan, Dynamic interaction of long suspension bridges with running trains, *Journal of Sound and Vibration* 237 (2) (2000) 263–280.
[10] Y.K. Cheung, F.T.K. Au, D.Y. Zheng, Y.S. Cheng, Vibration of multi-span bridges under moving vehicles and trains by using modified beam vibration functions, *Journal of Sound and Vibration* 228 (1999) 611–628.
[11] A. Matsuura, Study of dynamic behaviors of bridge girders for high-speed railway, *Journal of JSCE* 256 (12) (1976) 35–47.
[12] M. Klasztorny, Vertical vibration of a multi-span bridge under a train moving at high speed, *Proceedings of the EURODYN'99, Prague*, Vol. 2, Balkema, Rotterdam, 1999, pp. 651–656.
[13] H. Xia, N. Zhang, Dynamic analysis of railway bridge under high-speed trains, *Computers & Structures* 83 (2005) 1891–1901.
[14] G. De Roeck, A. Maeck, A. Teughels, Train–bridge interaction validation of numerical models by experiments on high-speed railway bridge in Antoing, *Proceedings of the MCCI'2000*, Delft University Press, The Netherlands, 2000, pp. 61–68.
[15] F.T. Wang, *Vehicle System Dynamics*, China Railway Press, Beijing, 1994.
[16] Y.B. Yang, J.D. Yau, Y.S. Wu, *Vehicle– Bridge Interaction Dynamics, with Application to High-Speed Railways*, World Scientific, Singapore, 2004.
[17] R.V. Dukkipati, *Vehicle Dynamics*, Alpha Science International Ltd, Pangourne, 2000.
[18] D.X. Zhang, *Vehicle– Track System Dynamics*, China Railway Press, Beijing, 1996.
[19] N. Zhang, et al., *Dynamic Analysis and Assessment of Several High-Pier Bridges on the Chengdu-Kunming Railway. Technical Report*, Northern Jiaotong University and Kunming Railway Bureau, 1998.

[20] H. Xia, et al., Analysis of resonance mechanism and conditions of train–bridge system, *Journal of Sound and Vibration* 297 (2006) 810–822.

He Xia the Professor, Beijing Jiaotong University, Beijing, China; Councilor of China Civil Engineering Society; Member of International Association for Bridge and Structure Engineering (IABSE). Born in 1951, Beijing, China; M.Eng.Sc. degree in 1984, Majoring in Bridge and Structural Engineering, Northern Jiaotong University, Beijing, China; Visiting scholar, Department of Civil Engineering, Catholic University of Leuven, 1989–1990; Research fellow, Department of Civil and Structural Engineering, The Hong Kong Polytechnic University, Hong Kong, China, 1999, 2000; Visiting Scholar, Institute of Railway Technology, Tokyo, Japan, 2002; and Visiting Fellow, School of Civil and Environmental Engineering, University of New South Wales, Sydney, Australia.